

LUMEDW - MEMR -- 1001. - SE

Dose Planning and Dose Delivery in Radiation Therapy

Tommy Knöös



**Lund University
Malmö 1991**

Dose Planning and Dose Delivery in Radiation Therapy

av

Tommy Knöös
Fil. kand., Mlm

Akademisk avhandling som för avläggande av doktorsexamen i medicinsk vetenskap vid medicinska fakulteten vid universitetet i Lund kommer att offentligas försvaras i kirurgiska klinikkens föreläsningssal, ingång 42, Malmö Allmänna Sjukhus, tisdagen den 28 maj 1991, kl 13.00 (precis).

Organization LUND UNIVERSITY Department of Radiation Physics Lund University, Malmö Allmänna Sjukhus S-214 01 Halmö, Sweden		Document name DOCTORAL DISSERTATION	
		Date of issue May 28, 1991	
		CODEN: ISRN 1016DW/DEHR--1001--SI	
Author(s) Tommy Kröös		Sponsoring organization	
Title and subtitle Dose Planning and Dose Delivery in Radiation Therapy			
Abstract A method has been developed for calibration of CT-numbers to volumetric electron density distributions using tissue substitutes of known elemental composition and experimentally determined electron density. This information have been used in a dose calculation method based on photon and electron interaction processes. The method utilizes a convolution integral between the photon fluence matrix and dose distribution kernels. Inhomogeneous media are accounted for using the theorems of Fano and O'Connor for scaling dose distribution kernels in proportion to electron density. For clinical application of a calculated dose plan, a method for prediction of accelerator output have been developed. The method gives the number of monitor units that has to be given to obtain a certain absorbed dose to a point inside an irregular, inhomogeneous object. The method for verification of dose distributions outlined in this study makes it possible to exclude the treatment related variance contributions, making an objective evaluation of dose calculations with experiments feasible. The methods for electron density determination, dose calculation and prediction of accelerator output discussed in this study will all contribute to an increased accuracy in the mean absorbed dose to the target volume. However, a substantial gain in the accuracy for the spatial absorbed dose distribution will also follow, especially using CT for mapping of electron density together with the dose calculation algorithm.			
Key words Radiotherapy, Dose Planning, Dose Calculation, Photon Beam Therapy, Dose Delivery, Output Factors, Convolution, CT-number, Electron Density			
Classification system and/or index terms (if any)			
Supplementary bibliographical information		Language English	
ISSN and key title		ISSN 91-628-0276-3	
Recipient's notes		Number of pages 40	Price
		Security classification	

Distribution by (name and address)

I, the undersigned, being the right owner of the abstract of the above-mentioned dissertation, hereby grant to all reference sources permission to publish and disseminate the abstract of the above-mentioned dissertation.

Signature _____

Date April 2, 1991 _____

From the Department of Radiation Physics, Malmö
Lund University

Dose Planning and Dose Delivery in Radiation Therapy

Tommy Knöös



Malmö 1991

Doctoral Dissertation
Lund University
Department of Radiation Physics
S-214 01 Malmö, SWEDEN

©Tommy I L Knöös (page 1-40)

ISBN 91-628-0276-3

CODEN: ISRN LUMEDW/MEMR--1001--SE

Printed in Sweden by Lund University, Reprocentralen 1991

To my family

Marlene, Patrik and Mikael

*When a man no longer wonders,
questions and plays,
then he is through with life.*

(Translated by the author from a
statement by
Hector El Neco, 1900-1984)

CONTENTS

INTRODUCTION	6
AIM OF THE PRESENT STUDY	9
CALIBRATION OF CT-SCANNERS	9
Tissue Substitutes	10
Determination of Electron Density	13
Determination of Hounsfield number	15
Hounsfield Number Versus Electron Density	16
DOSE CALCULATION ALGORITHMS	16
Algorithms Without Scatter Modelling	17
Algorithms with Scatter Modelling	17
Convolution Procedures for Dose Calculation	18
Convolution in Inhomogeneous Media	20
Effects of Spectral Variations	21
TREATMENT VERIFICATION	23
APPLICATION OF A DOSE PLAN	25
Modelling of Energy Fluence from an Accelerator	26
Calculation of Monitor Units	27
GENERAL SUMMARY	30
CONCLUSIONS	31
FUTURE DEVELOPMENT	32
Consistency When Reporting Absorbed Dose	32
Dosimetric Methods Used for Verification	33
Multileaf Collimator	33
On-line Verification	33
3D-Treatment Planning	34
Treatment Execution	34
ACKNOWLEDGEMENTS	35
APPENDIX	36
REFERENCES	37

This thesis is based on the following papers, which will be referred to by their Roman numerals:

- I** Knöös T, Nilsson M, Ahlgren L, A method for conversion of Hounsfield number to electron density and prediction of macroscopic pair production cross-sections, *Radiother Oncol*, 5, 337-345, 1986.
- II** Nilsson M, Knöös T, Application of Fano's theorem in inhomogeneous media using a convolution algorithm, Submitted to *Phys Med Biol*, 1991.
- III** Knöös T, Ahlgren L, Nilsson M, Comparison of measured and calculated absorbed doses from tangential irradiation of the breast, *Radiother Oncol*, 5, 81-88, 1986.
- IV** Knöös T, Jónsdóttir T, Wittgren L, Nilsson M, Ahlgren L, Comparison of X-ray qualities for AP treatment of the thorax, Submitted to *Radiother Oncol*, 1989.
- V** Knöös T, Wittgren L, Which depth dose data should be used for dose planning when wedge filters are used to modify the photon beam? *Phys Med Biol*, 36, 255-267, 1991.
- VI** Ahnesjö A, Knöös T, Montelius A, Application of the convolution method for calculation of output factors for radiotherapy beams, Submitted to *Med Phys*, 1990.

Preliminary reports have been presented at the following international meetings:

- i** Knöös T, Jónsdóttir T, Ahlgren L, Nilsson M, Comparison of absorbed dose to the lung and untreated breast using symmetrical and asymmetrical collimators for tangential treatment of breast cancer, In: Proceedings of the Fifth Varian European Clinac Users Meeting at Flims, Switzerland, Varian International AG, Switzerland, p 21-23, 1987.
- ii** Knöös T, Nilsson M, Calculation of 3D dose distributions for photons in inhomogeneous media, In: 'The use of computers in radiation therapy', Proceedings Ninth International Conference on the Use of Computers in Radiation Therapy, Ed by Bruinvis I A D, North-Holland, p 111-114, 1987.
- iii** Wittgren L, Knöös T, Need of special depth dose data for wedged photon beams, In: Programs and Abstract 9th ESTRO-meeting, Montecatini Terme, Italy, p 409, 1990.

INTRODUCTION

Radiation therapy is used for treatment of approximately every second patient with cancer when *in situ* cancers of skin and cervix are excluded (see figure 1). Curatively intended radiotherapy is given to one out of two patients. Half of these, however, will fail as a result of either distal or local recurrences. This equals approximately 16 % of all patients receiving radiation therapy.

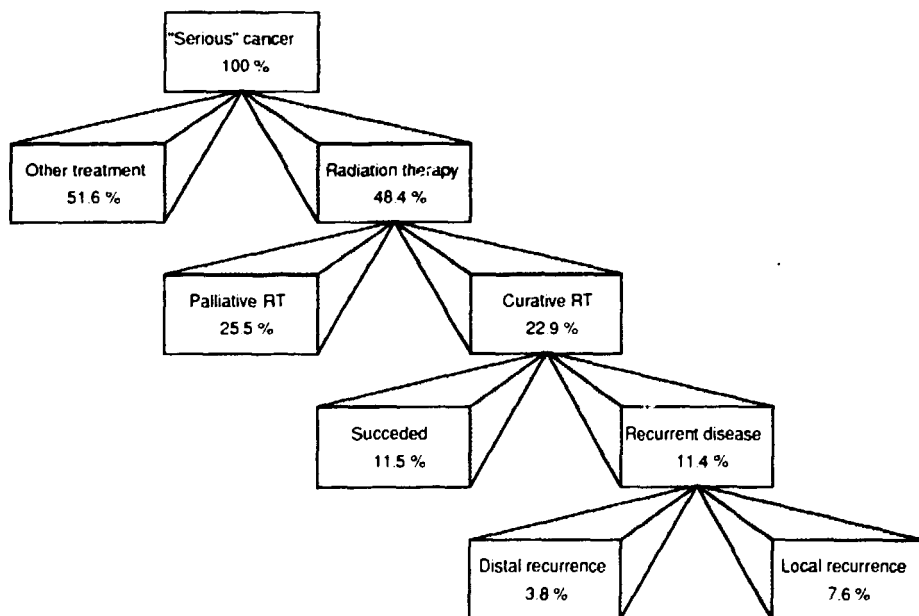


Figure 1: Estimates of the annual number (%) of new patients diagnosed with malignant disease and the number of patients receiving radiation therapy. The box representing radiation therapy includes also combinations with other modalities e.g. chemotherapy and surgery. The figures are based on 1980 cancer incidence in the United States (DeVita, 1983).

An improved local treatment using advantageous and reproducible dose distributions will make it possible to give a higher absorbed dose to the clinical target volume without exceeding the tolerance of surrounding normal structures. This will lead to a) an increased survival probability, b) a decrease in treatment related morbidity probability and c) a decrease in frequency and severity of complications (Suit *et al.* 1988, Suit *et al.* 1989). A dose distribution

is considered advantageous if the treated volume¹ is reduced close to the planning target volume and if the discrepancy between the two volumes is minimized (see figure 2).

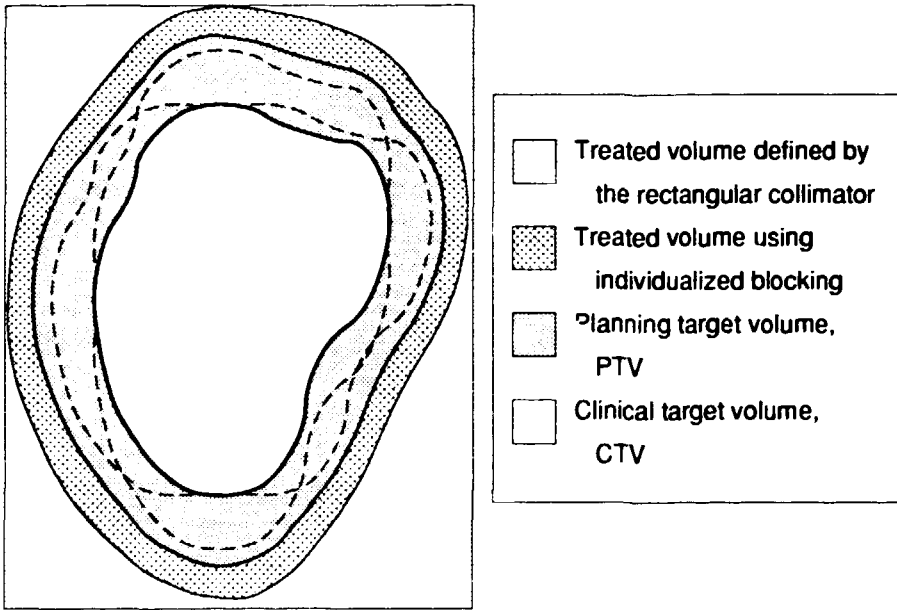


Figure 2: The clinical target volume, CTV, which may move due to respiration etc, includes the tumour and other tissues which are to be irradiated to a certain prescribed absorbed dose. The CTV is enclosed by a static planning target volume, PTV, which is the foundation for the dose planning and the determination of beam orientation etc. The volume enclosing the PTV is the treated volume which is dependent on the treatment technique chosen. Minimizing the treated volume by using, for example, individualized blocks instead of the much larger rectangular field from the accelerator for beam shaping is an example of a way to improve a dose distribution.

The accuracy in absorbed dose required for local tumour control using radiation therapy was discussed by ICRU (1976) where it was recommended that, "an accuracy of $\pm 5\%$ in the delivered absorbed dose to a target volume should be obtained if the eradication of the primary tumour is sought". It has been pointed out, based on a radiobiological model, that an increased variance of the absorbed dose inside a target volume will decrease the local control (Brahme, 1984, Brahme *et al.* 1988). Additionally, an increased uncertainty in the stated mean absorbed dose will decrease the slope of the observed tumour control probability curve. If the standard deviation of the observed tumour

¹The nomenclature used follows the recommendations of ICRU (1978), Wambersie *et al.* (1989) and Landberg (1991) for treatment reporting and ICRU (1980) for physical quantities.

²The ICRU has not explicitly defined what this figure represents (range, 1 SD etc).

control probability should be less than 5 % to allow evaluation of various treatment regimes etc, the variation in absorbed dose must be less than 5 % and in many situations less than 3 % (Brahme, 1984, Brahme *et al.* 1988).

Dutreix (1984) reported that a change of 10 % in absorbed dose to the tumour significantly can change the probability of tumour control as well as the complication probability. Dutreix stated that an overall uncertainty of the delivered target dose should be less than ± 5 %. Mijnheer *et al.* (1987) discussed the accuracy needed to maintain a high tumour control and gave a requirement of 3.5 % (1 SD). These figures are comparable if it is assumed that the ranges given (± 5 %) are related to a variation of approximately 1.5 SD.

From these studies, it can be concluded that *the mean absorbed dose inside a target volume should be known within 3 % (1 SD) and the variation over the volume should not exceed 3-5 % (1 SD)*. These requirements are based on clinical observations of tumour control and complication frequencies. In absorbed dose figures reported, an uncertainty is involved due to what type of patient data, dose calculations etc that have been used. Another, perhaps the most important, source of error in all clinical data is the different methods for specification and reporting of treatments.

Many studies have been published regarding dosimetric accuracy in a fixed geometry with irradiation of a water phantom (reference dosimetry) (Svensson 1971, Bjärngård *et al.* 1980, Johansson *et al.* 1982, Johansson *et al.* 1986, Svensson *et al.* 1990). These studies clearly indicate that the given absorbed dose is generally in close agreement with the stated absorbed dose. However, certain variations exist, and are not only found between the different centres but also within departments, especially between treatment machines of different design and with different radiation quality (Johansson *et al.* 1982). Short-term variations for individual machines also exist and are revealed by daily or weekly measurements (Purdy *et al.* 1987, Knöös, 1988). An accuracy of the absorbed dose under reference conditions of 2.5 % (1 SD) for photons and 2.8 % for electron beams has been reported (Andreo, 1990).

In conclusion, more curative treatments must be given in the future especially to patients with small target volumes having a high probability of complete cure. Therefore, the local tumour control must be as high as possible for these patients. The hypothesis is that a decreased uncertainty of the delivered dose will result in an increased therapeutic gain due to higher local tumour control or lower complication frequencies.

The accuracy in absorbed dose which is achievable under reference conditions is comparable to the clinically required accuracy. In optimal situations, for example, an opposed field technique applied to a homogeneous patient, the accuracy can be 4 % (Mijnheer *et al.* 1987). Therefore, when all methods used are applied to clinical conditions, they should only affect the accuracy marginally.

AIM OF THE PRESENT STUDY

The aim of this study was to investigate some factors important to achieving an increased *accuracy* of the absorbed dose delivered to the patient.

The main objectives were:

- ☛ To develop a method for mapping of electron density distributions and to apply this information in a dose calculation method based on photon and electron interaction processes.
- ☛ To develop an objective dosimetric procedure for verification of dose distributions.
- ☛ To increase the accuracy in mean absorbed dose to the target volume when applying a calculated dose plan.

CALIBRATION OF CT-SCANNERS

Since the introduction in the early seventies, the use of computerized tomography (CT) for radiotherapy planning has increased the accuracy both for geometric volume definitions (Goitein, 1982, Dobbs *et al.* 1983) and for dose calculations. The CT-scan consists of a distribution of attenuation values relative to water (Hounsfield Numbers, HN or CT-numbers) which can be related to the linear attenuation coefficients (μ). The linear attenuation coefficients are dependent on the electron density and the elemental composition. The relation between Hounsfield number and the linear attenuation coefficient for monoenergetic X-rays (73 keV) and water equivalent tissues is:

$$\mu_{tissue} = \mu_{water} \cdot \left(1 + \frac{HN}{1000} \right)$$

However, in practice, polyenergetic X-rays are used and the energy distribution will vary from point to point due to beam hardening. Corrections for beam hardening are often included in the reconstruction algorithms but all tissues are assumed to be water equivalent. Scattered radiation produced within the scanned volume will also contribute to the resulting image. Therefore, the evaluation of the equation above can not be done accurately. The use of samples with known *elemental composition* and *electron density* will, however, allow a conversion of CT-numbers to electron density (electrons/cm³)¹.

Tissue Substitutes

Materials with an atomic composition as close as possible to the simulated tissues were used. The elemental compositions for muscle, lung, average bone and cortical bone were taken from ICRU (1989). Lung tissue was simulated using cork, wood and poly-urethane foam. Bone substitutes using an epoxy resin, CB4² with additionally CaHPO₄·2H₂O, were mixed according to White *et al.* (1977). The usefulness of the materials as tissue substitutes with respect to their absorption characteristics can be estimated using an effective atomic number approach (White, 1977, White and Constantinou, 1982):

$$\bar{Z} = \left\{ \sum_i \epsilon_i \cdot Z_i^{m-1} \right\}^{1/(m-1)}$$

where Z_i is the atomic number and ϵ_i is the relative number of electrons of element i in the substitute according to:

$$\epsilon_i = \left\{ \frac{\omega_i N_A Z_i}{A_i} \right\} \cdot \left\{ \sum_i \frac{\omega_i N_A Z_i}{A_i} \right\}^{-1}$$

N_A is Avogadro's number, A_i is the atomic mass and ω_i is the relative weight by mass of element i . The exponents m , valid for atomic number 5 to 15, were chosen from White (1977). The mass attenuation coefficient for a specific photon interaction process at a certain energy can then be estimated using:

$$\left[\frac{\mu}{\rho} \right]_{process} \propto \rho_e \cdot \bar{Z}^{m-1}$$

¹ Electron density is consistently expressed as electrons per unit volume relative to that for water throughout this thesis except where specially stated.

² A mixture of Araldite MY 750® and XD 716® for the hardening. Both substances are available from Ciba-Geigy.

where ρ_e is the electron density in electrons/g for the substitute. The quality of the substitutes was evaluated using a *quality index* defined as the ratio between the estimated mass attenuation coefficients for the substitutes and the tissue in question. This was made for photon interaction processes of interest.

Table I: Ratios between mass attenuation coefficients for some common tissue substitutes at different photon energies (150 keV for photoelectric absorption and coherent scattering, 1 MeV for incoherent scattering and 5 MeV for pair production). Ratios were calculated according to Berger and Hubbell (1987). The figures enclosed by parentheses were estimated using the effective atomic number model with the exponents (m) given. Elemental compositions for tissues are from ICRU (1989).

Photon process	Photoel. τ/ρ m=4.78	Coherent σ_{coh}/ρ m=2.68	Incoherent $\sigma_{\text{incoh}}/\rho$ m=1	Pairprod. κ/ρ m=1.96
<i>Muscle tissue substitutes</i>				
Water	0.93 (0.93)	1.03 (1.04)	1.01 (1.02)	1.03 (1.03)
Alderson	1.08 (1.14)	0.77 (0.76)	0.99 (0.98)	0.86 (0.85)
Mix D	1.07 (1.14)	0.77 (0.79)	1.03 (1.05)	0.84 (0.86)
Paraffin	0.29 (0.31)	0.61 (0.64)	1.04 (1.09)	0.77 (0.80)
PMMA	0.54 (0.53)	0.80 (0.78)	0.98 (0.96)	0.89 (0.87)
Polystyrene (white)	1.06 (1.08)	0.76 (0.74)	0.97 (0.95)	0.84 (0.82)
Polystyrene (clear)	0.34 (0.32)	0.71 (0.65)	0.91 (0.96)	0.84 (0.79)
Polyethylene	0.30 (0.31)	0.62 (0.64)	1.04 (1.08)	0.77 (0.80)
<i>Lung tissue substitutes</i>				
Alderson lung tissue	1.66 (2.25)	0.78 (0.76)	0.96 (0.92)	0.86 (0.83)
<i>Average bone substitutes</i>				
Aluminium	1.85 (1.58)	2.03 (1.75)	0.89 (0.79)	1.57 (1.40)
CB4 + 5 % CaHPO ₄	0.28 (0.28)	0.66 (0.66)	0.99 (0.99)	0.82 (0.83)
CB4 + 10 % CaHPO ₄	0.42 (0.41)	0.73 (0.72)	0.99 (0.98)	0.84 (0.86)
Plaster of Paris	3.10 (2.91)	2.02 (1.89)	0.95 (0.89)	1.53 (1.43)
PTFE (Teflon*)	0.37 (0.31)	0.94 (0.82)	0.89 (0.79)	1.01 (0.90)
<i>Cortical bone substitutes</i>				
Aluminium	0.72 (0.64)	1.18 (1.07)	0.94 (0.88)	1.15 (1.08)
CB4 + 60 % CaHPO ₄	0.70 (0.70)	0.81 (0.82)	1.02 (1.03)	0.79 (0.90)
Plaster of Paris	1.20 (1.18)	1.17 (1.15)	0.99 (0.98)	1.11 (1.10)
PTFE (Teflon*)	0.14 (0.13)	0.55 (0.50)	0.93 (0.87)	0.74 (0.69)

The validity of this *quality index* has been evaluated using calculated mass

attenuation coefficients¹. A similar index is calculated for these coefficients and the two quality indices were compared. An average deviation of +1.6 % (+0.1 % to +3.2 %)² was found (positive value indicates a larger value for the effective atomic number method), see also table I. Thus, especially when cross section data is unavailable, evaluation of a certain substitute can be done using the effective atomic number method.

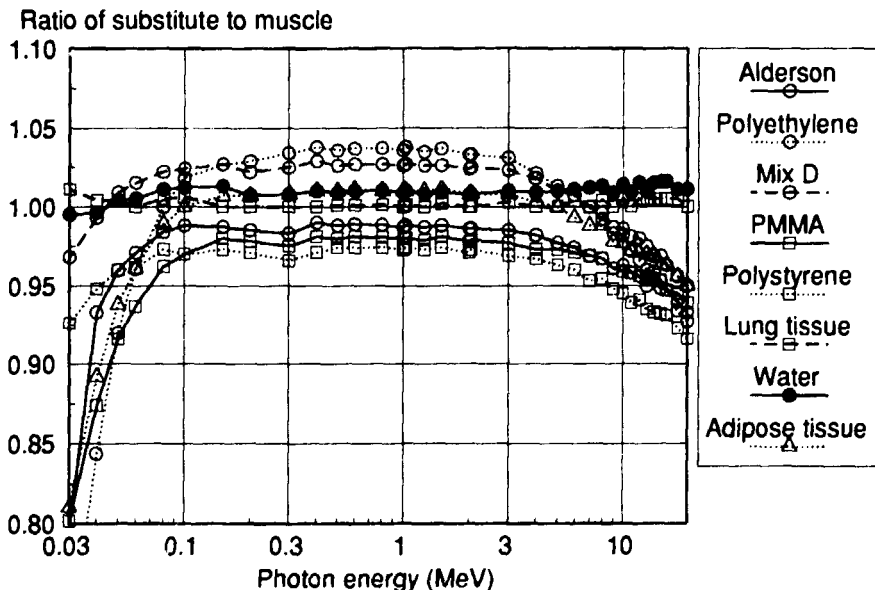


Figure 3: Total mass attenuation coefficient (μ/ρ) ratios for muscle substitutes. Mass attenuation coefficient ratios for lung and adipose tissues to muscle is also shown. The graphs were based on cross section data from Berger and Hubbell (1987).

Further on, it was assumed that all human tissues with electron densities less than that of muscle could be represented by muscle of lower physical density. A test of this assumption was accomplished using the ratio of mass attenuation coefficients, (μ/ρ), for lung and adipose tissue to that for muscle. These ratios together with ratios for some common tissue substitutes, including the CB4 epoxy resins, are shown in figure 3 and 4. Only minor difference in total mass attenuation coefficient between lung and muscle can be seen for the energy range studied. However, adipose tissue differs from muscle but the differences for energies between 100 keV and 5 MeV is negligible (< 1 %).

¹All mass attenuation coefficients were calculated for single elements and compounds using a computer program XCOM by Berger and Hubbell (1987). The program uses stored cross sections for element 1 to 100 and from these data, a compilation of cross sections for any compound can be obtained.

²A 95 % confidence interval.

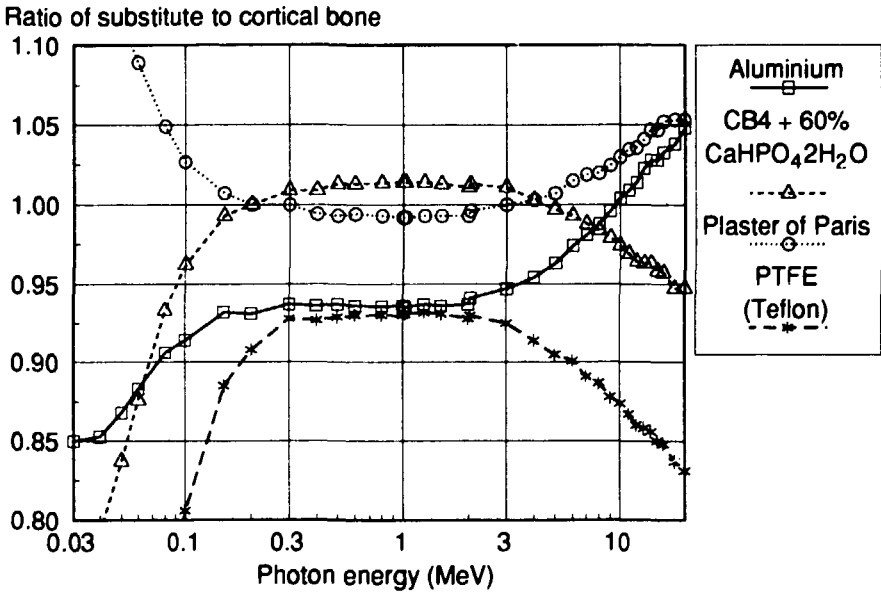


Figure 4: Total mass attenuation coefficient (μ/ρ) ratios for *cortical bone* substitutes. The graphs are based on cross section data from Berger and Hubbell (1987).

Many of the substitutes, including those used in the Alderson phantom as lung and muscle, are well suited to dosimetry. However, some of them should be used with care in energy ranges where inelastic scatter is not the dominating photon interaction process. It is also evident that water is consistently the most suitable muscle substitute available for all photon energies considered. The bone substitutes used (CB4 based epoxy resins) are all suitable for use in radiotherapy, both as substitutes for cortical bone as for average bone. Compared with other substitutes, for example Al and PTFE, the CB4 based substitutes simulates cortical bone better.

Determination of Electron Density

The cross section per free electron for incoherent scatter of photons is given by the Klein-Nishina relation (Evans, 1955). When electrons are bound to an atom, the cross section per atom is given by the product of the electronic cross section and an incoherent scattering function which is energy and atomic number dependent (Hubbell *et al.*, 1975). In figure 5, the atomic cross sections divided by the atomic number, Z , are shown. For the energy region where the curves coincide, the incoherent scattering function is equal to Z , thus the quotient is

equal to the electronic cross section for a free electron. At lower energies, however, the scattering function is less than Z . Therefore, the Klein-Nishina electronic cross section can be used for incoherent scattering for elements present in human tissues for energies above approximately 0.2 MeV. The linear attenuation coefficient at these energies is close to the electronic cross section, σ_e^1 , times the number of electrons per unit volume i e the electron density, ρ_e (electrons/cm³).

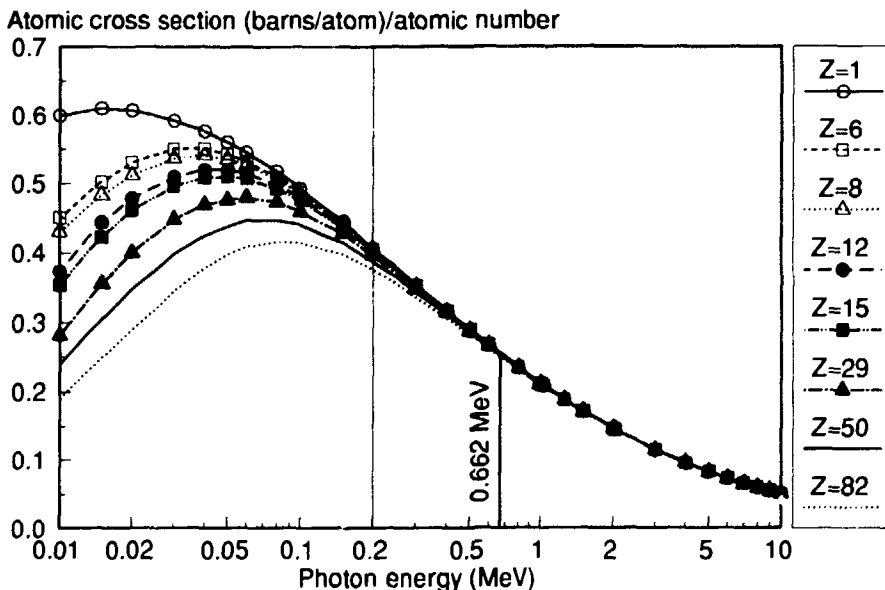


Figure 5: The atomic cross-section σ_a (barns/atom) for incoherent scattering divided by the atomic number Z for photon energies between 0.01 to 10 MeV. The curves gives that the atomic cross section is approximately proportional to the atomic number for energies larger than 0.2 MeV, at least for Z less than 15. In the low energy region, the binding of the electrons to the atomic nucleus will result in a lower atomic cross section than that given by the electronic cross section σ_e times Z .

For the soft and bone tissue substitutes discussed, the electron density was experimentally determined (paper I). Cylindrical samples were used (length $l=4.5$ cm, diameter 2.0 cm). The transmitted fraction, N/N_0 , for 662 keV γ -photons was determined in a narrow beam geometry. The absolute electron density was evaluated using the following equation:

$$\rho_{e,i} = -\frac{\ln(N_i/N_0)}{\sigma_e \cdot l}$$

¹⁾ $\sigma_e=0.2575$ barns/electron at 662 keV

This equation will overestimate the electron density with 0-0.6 % due to the small contribution from photoelectric absorption (0.15 % for cortical bone) and coherent scattering (0.41 %). The overestimation will be largest for the samples with the largest proportion of elements with high atomic number. Since, in most situations, the electron density required is that relative to water, the quotient between the logarithms of the transmitted fractions for a sample and water can be used instead:

$$\rho_{e,i} = \rho_{e,water} \cdot \frac{\ln(N_i/N_0)}{\ln(N_{water}/N_0)}$$

The experimentally determined electron densities are in close agreement to calculated values — water (-0.1 %), ice (-1.7 %), Alderson (-2.4 %), PTFE (-0.1 %), PMMA (-1.9 %) and polystyrene (-1.7 %). The uncertainty in the experimentally determined electron density is due to differences in length of the samples, mean length 4.51 cm ± 0.02 cm (1 SD)¹, uncertainty in the physical density (g/cm³) and the counting statistics for the transmission measurements. At least 50000 counts at each measurement were integrated, thus 1 SD is less than 0.5 %. The net counts for the case when no sample were present (N_0) showed a variation of 1.2 % (1 SD) during the experiment. Therefore, the total uncertainty in the measured electron density is estimated to be less than 1.5 % (1 SD).

Determination of Hounsfield number:

A water sample and four substitute samples at a time, were placed in a cylindrical polystyrene phantom (diameter 20 cm). CT scanning was made under identical conditions as those for radiotherapy patients. The mean Hounsfield numbers with standard deviations (SD) were determined in circular regions (diameter 1.3 cm) with the centre coinciding with the centre of the samples. The standard deviation (SD) for the Hounsfield numbers were 3-5 units for the homogeneous samples which increased to 10 to 60 units for inhomogeneous samples i.e. cork and wood. Perturbations on the result from beam hardening could be neglected because CT-values for five water samples at various positions in the phantom gave the same reading.

¹) For water, a length of 6 cm was used.

Hounsfield Number Versus Electron Density

A linear relationship between Hounsfield number and electron density was found to be valid up to about 150 HN for materials with an atomic composition similar to muscle. From here upward, the higher atomic number in bone tissues affects the attenuation, resulting in a less steep relation (cf figure 3 in paper I).

The *spatial resolution* requirement on the electron density distribution matrix for use in dose planning can be found using a similar approach as Goitein (1982) assuming an approximate dose gradient on the radiation beam axis in an X-ray beam of 5 %/cm. Thus, each pixel with length p (cm) will attenuate the primary photons $5 \cdot p$ %. Pixel dimensions of less than 50 cm per 256 pixels¹ i.e. ≤ 0.2 cm are common. The attenuation of the photon beam will therefore be in the order of 1 % per pixel. If an error in the calculated dose, using conventional dose planning algorithms, of 1 % for depths larger than the build up depth is accepted, an error of not more than one pixel in the delineation of the patient outline is required. For the same accepted uncertainty in absorbed dose, a less careful outlining of regions of lower density may be accepted.

The required accuracy for the *electron density* is determined by the requirement for the radiological depth. Using the same approach as above gives that this depth should be known within 0.2 cm. It has been shown (Goitein, 1982) that the statistical uncertainties in the CT-number (electron density) are of no practical concern for the calculation of radiological depth. However, systematic errors can not be eliminated, for example effects of contrast media and movements.

For beam qualities with considerably steeper dose gradients, for example electrons, other requirements on spatial resolution and electron density may be implied.

The use of the physical quantity electron density, compared with less accurate estimations of for example lung density have substantially improved the accuracy in the calculations. The most important achievements are accurate spatial distribution and the possibility to use more sophisticated calculation methods.

DOSE CALCULATION ALGORITHMS

Clinically used dose planning systems have until recently used algorithms for photons which make use of empirically determined inhomogeneity corrections. The methods in use today can be grouped according to their handling of scatter.

¹⁾ Matrix sizes used in most CT scanners today are often equal to or larger than 256².

Algorithms Without Scatter Modelling

In this group of algorithms, *effective attenuation, isodose shift, tissue air ratios, effective source skin distance* (ICRU, 1976) only the radiological depth for the calculation of absorbed dose is considered. More or less sophisticated versions exist — approximations of homogeneous media, regional corrections or pixel by pixel corrections. A better method was introduced with the algorithm by Batho (1964) where the *position* of the inhomogeneity along the ray also is considered.

The resulting dose distributions from these models can in some clinical cases differ up to 20 % from measurements, especially in low density media irradiated with narrow ($5 \times 5 \text{ cm}^2$) high energy photons beams (Mackie *et al.* 1985a). Deviations of the same magnitude between measurements and calculations were found (paper III) for a tangential beam geometry using the effective attenuation method. Of these methods, the Batho method estimates the absorbed dose with the highest accuracy. Lulu and Bjärngard (1982), have extended the Batho algorithm to account also for the lateral extension of inhomogeneities.

Algorithms with Scatter Modelling

The next group of methods all use the radiological depth to determine the primary dose component but also account for scatter produced in the irradiated volume.

The *Equivalent Tissue Air Ratio*, ETAR algorithm (Sontag and Cunningham, 1978) relies on a calculation of an effective homogeneous density which is assigned to each point using weighting factors applied to the surrounding points (voxels). Geometric dimensions are scaled according to O'Connor (1957) (see below). An accuracy of $\pm 3 \%$ (Sontag and Cunningham 1978) can be expected in most cases, however, in some situations, the deviation for the ETAR method can increase, for example for tangential beams, where deviations up to 5 % have been found (Wong and Henkelman, 1983).

The *differential Scatter Air Ratio* method, dSAR (Beaudoin, 1968, Cunningham, 1972) accounts for variations in fluence due to the radiological depth and density at the scatter point. The dSAR method utilizes *measured* beam data from which scatter air ratios differentiated in depth, distance and angle are calculated. All scatter is handled as single scatter which in situations with irradiation of large homogeneous non-unit density media (lung tissues) still may give inaccurate results (Cunningham, 1982, Wong and Henkelman, 1983).

The *Delta Volume* method, DV (Wong and Henkelman, 1983) is similar to the dSAR method, however, the *calculated* first scatter is *augmented* to include the second generation of scatter. This *residual* scatter is ascribed to a correction term such that the final dose distribution using the augmented scatter agrees with measurements. The accuracy for the DV-method is further increased, especially for large non-unit homogeneous geometries.

In general, none of the methods discussed deals with the lack of electronic equilibrium for narrow beams of high energy X-rays in low density media. All these models assume that the energy transferred to electrons is absorbed locally i.e. the collision kerma is equal to the absorbed dose.

Convolution Procedures for Dose Calculation

The limited accuracy of the methods described has initiated many studies on methods which are based on physical principles. The best choice is the Monte Carlo method where the full 3D description of the patient is used and all basic interactions for photons and electrons are considered. The method has, however, one very limiting drawback — the calculation time. Presently other methods have to be used until the speed of computers reach a level where Monte Carlo based dose planning can be used interactively:

Mathematically, a convolution process can be written as the following integral:

$$h(x) = \int f(x') \cdot g(x - x') dx'$$

or in short

$$h(x) = f(x) \otimes g(x)$$

The function f is convolved with the kernel function g to give the resulting function h . Applied to dose calculations, f and g can be considered as the photon fluence distribution and the absorbed dose distribution per unit fluence around an interaction site, respectively. Then, h will represent the final dose distribution. This integral can be solved using Fourier transforms where the convolution integral is replaced by the inverse Fourier transform of the product between the forward transforms of f and g .

This approach is fundamental in the studies by Boyer who used a Fast Fourier Transform (FFT) to solve the convolution integral for the final dose distribution (Boyer, 1984, Boyer and Mok, 1985). However, if the kernel function g varies with x , for example the dose distribution kernel depends on the electron density, a spatial convolution integral has to be solved instead.

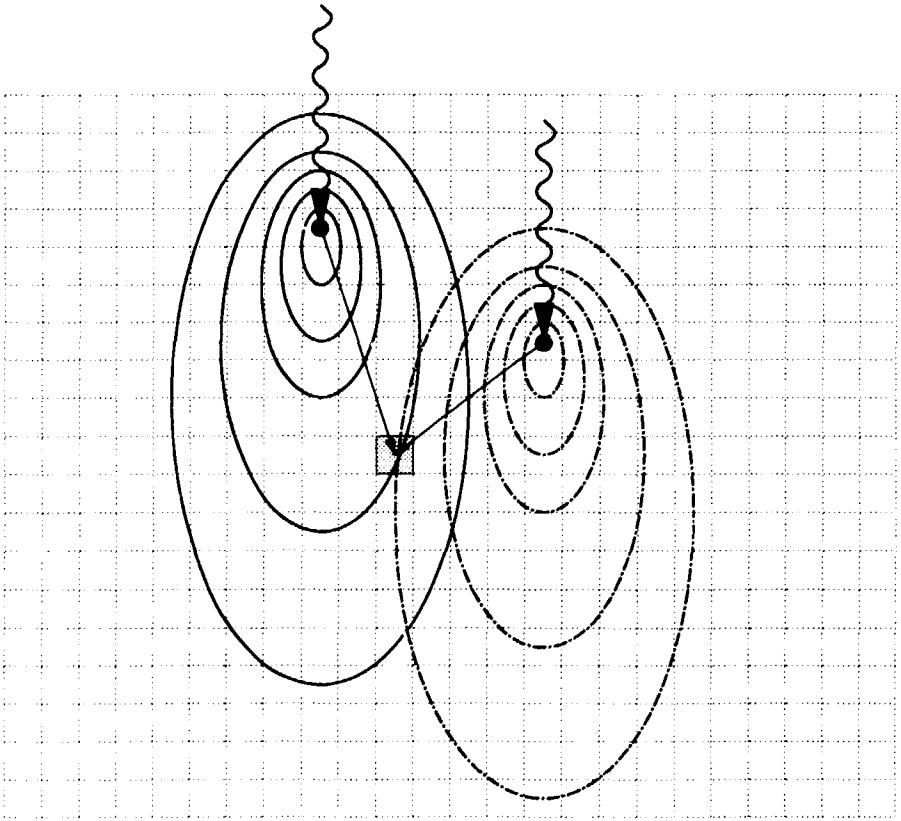


Figure 6: A matrix of photon fluence (dotted lines) is *convolved* with a dose distribution kernel, shown as isolevels (solid lines and broken lines) representing the pattern of absorbed dose around an interaction point (●). The absorbed dose to the shaded voxel (dose point) is determined as the fluence at the interaction point times the level of the kernel at the dose point. This is repeated for all interaction sites (only two is shown for clarity) to get the total absorbed dose to a single voxel.

In figure 6, the principle of convolution applied to dose calculations in external beam therapy is outlined. The dose distribution kernels used, which includes electrons released in the first interaction as well as single and multiple scattered photons, are generally calculated using Monte Carlo simulations but analytical methods are also applicable. The convolution method in paper II utilizes both approaches, Monte Carlo¹ for primary electrons produced by compton or pair production processes in the first interaction and analytical methods for scattered radiation.

¹Using an implementation of the model presented by Raeside (1976).

Convolution in Inhomogeneous Media

Inhomogeneous media can be included in the convolution integral either using a large number of dose distribution kernels, one per density, or a single kernel combined with the following *scaling* theorems:

"In a medium of a given composition exposed to a uniform flux of primary radiation (such as X-rays or neutrons) the flux of secondary radiation is also uniform and independent on the density of the medium as well as of the density variations from point to point." (Fano, 1954)

"In a given irradiation system the ratio of scattered photons to primary photons remains unchanged when the density of the irradiated material is changed if all the linear dimensions of the system are altered in inverse proportions to the change in density." (O'Connor, 1984¹)

Density in this context should be interpreted as interaction sites per unit volume, e.g. electron density for incoherent scattering of photons. It is also assumed that the amount of secondary radiation produced at a point is proportional to the local number of interaction sites. These theorems were also applied in the ETAR method (Sontag and Cunningham, 1978).

Mackie *et al.* (1985b) used convolution kernels calculated for several densities. A similar approach using kernels for only a *single* density combined with the scaling theorems has been applied by e.g. Mohan *et al.* (1986), Ahnesjö *et al.* (1987) and Knöös and Nilsson (1987).

The use of a *discrete* single density kernel which is scaled during calculation may give errors in the final dose distribution. This is most pronounced in kernels where large changes in the gradient over the voxel is present i.e. in the centre of the primary electron dose distribution kernel. The collapsed cone convolution algorithm (Ahnesjö, 1989) and the convolution method given in paper II have both overcome these difficulties.

Thorough studies of the scaling process showed that large errors were introduced for the central voxel value due to the discrete description of the kernel (paper II). Correcting the kernel value in the interaction point during convolution eliminated these scaling errors. The correction factors, as a function of density were determined for 2.5 and 10 MeV monoenergetic photons. Similar values were found for both energies. The correction factors were only applied to the electron dose distribution kernel. In the photon scatter kernels, the gradient alterations over the voxel closest to the centre are small and no correction was needed.

¹The relationship between densities and geometries of the irradiated volumes was first presented by O'Connor (1957).

The primary photon fluence distribution was found from ray tracing through the three dimensional volume. The dose distribution kernels were superposed onto this matrix and scaling of distances and kernel values was accomplished using the scaling theorem. The basis for scaling of the kernels was the mean electron density between the interaction and dose deposition voxels.

Dose distributions in a complex slab geometry and a schematic mediastinum-like geometry were calculated using the developed method. Comparisons were made with dose distributions calculated¹ with the EGS4 Monte Carlo code (Nelson *et al.* 1985).

The results from the developed algorithm (paper II) are in close agreement to the Monte Carlo results. The slab and the mediastinum-like geometries are rigorous tests of the scaling theorem. The use of a correction factor applied to the central kernel value seems to be useful for convolution methods when density scaling is made. The monoenergetic photons and dose distribution kernels as used with the correction method implies that the algorithm should be as least as accurate for polyenergetic X-rays. The gradients present in the dose distribution kernels, especially the primary electron kernels, are less steep for X-ray spectra (Metcalf *et al.* 1989). The method used is based on dose distribution kernels calculated with a rather simple Monte Carlo model and analytical methods. Still, the results in the final dose distributions agree well with the EGS4 results.

The convolution method includes ray tracing of scattered photons and, which is of significance, the energy transport by electrons away from the first interaction site. Modelling of electronic disequilibrium is therefore included.

Furthermore, the method gives the resulting dose distribution in absolute dose i e the absorbed dose per incoming photon fluence unit ($\text{keV g}^{-1} \text{cm}^2$ or pGy cm^2). The calculated absorbed dose is therefore traceable back to the photon fluence impinging on the irradiated object. If the photon fluence from an accelerator is determined, the resulting absorbed dose will be possible to predict with high accuracy. However, this fluence will be influenced by scatter produced in the treatment head and in the traversed air column. Also the design of the monitor chamber in the accelerator has to be considered.

Effects of Spectral Variations

One approximation which still is used by the convolution/superposition methods is that the ray tracing of primary photons uses one single effective attenuation coefficient. The problems associated with different photon spectra

¹These simulations have been performed by Anders Ahnesjö at Stockholm University and supplied for this study which hereby is acknowledged.

in different parts of the beam and beam hardening along the ray have not yet been accounted for. Neglecting computation time, these problems can be dealt with, if the ray tracing process accounts for the varying X-ray spectra and spectral hardening. For example, Ahnesjö (1989) and Metcalfe *et al* (1990), use X-ray spectra during the ray tracing but apply, during convolution, invariant polyenergetic dose kernels compiled from several monoenergetic kernels. The methods have therefore the potential to consider the spectral variations within the beam for the primary photons. A similar approach was applied by Boyer *et al* (1989) repeating the FFT convolution for several monoenergetic photons which increased the computation time in proportion to the number of convolutions.

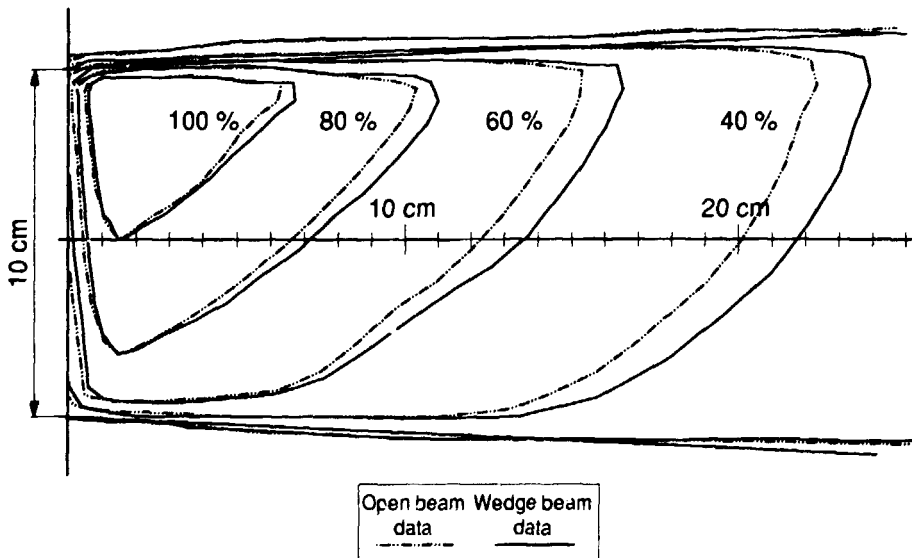


Figure 7: Isodose distributions in a homogeneous unit density medium, reconstructed from depth dose curves and beam profiles. The calculations are based on measured beam data for an open beam and a beam with a 45° wedge filter, respectively. The beam quality is 6 MV and the material in the wedge is lead. The field size is 10 x 10 cm².

The use of a single attenuation coefficient will also introduce errors when wedge filters are modelled. The magnitude of such errors is discussed in paper V. The slopes of the depth dose curves decrease when wedges are used due to *beam hardening*. The material, geometry and thickness of the wedge filters and the accelerating potential of the accelerator influences the magnitude of the beam hardening effect.

In figure 7, dose distributions calculated using measured depth dose data for open and wedged beams are shown. The discrepancies shown are such that all efforts in improving other steps in the calculations will be effectively hidden if the change in depth dose due to spectral variations is not considered.

To account for spectral hardening from attenuation in filters (wedge and compensators), the ray tracing process should include the filters and use a polyenergetic beam. It will then be possible to model both beam hardening in the filters and the change in fluence distribution over the beam.

TREATMENT VERIFICATION

Validating dose calculations using experimental methods is a cumbersome and tedious work and in some situations dosimetric problems will arise. Therefore, Monte Carlo techniques are common for verification. The ultimate goal for verification should be to determine the absorbed dose distribution *in vivo* for the actual treatment. In papers III and IV a method has been explored using thermoluminescent dosimeters (TLD) which were positioned in a human like phantom (Alderson Rando Phantom).

The phantom went through all planning stages including CT-scanning and simulation. Each treatment technique studied was set up and executed four times. The dose data acquired using LiF thermoluminescent dosimeters (TLD-100, $0.3 \times 0.3 \times 0.9 \text{ cm}^3$) was statistically analysed in order to separate the *dose distribution* and *repetition* variances from the *total* variance. The distribution variance, which is assumed to be independent of the repetition variance, is an estimation of the actual variation of the dose distribution inside the phantom. As a consequence, the estimated dose distribution variance can be compared with the variance in calculated dose distributions.

The validity of the method including the statistical separation of variances has been tested using a cubic polystyrene phantom ($30 \times 30 \times 30 \text{ cm}^3$). Five treatment set-ups were made. A $20 \times 20 \text{ cm}^2$ field with a SSD of 100 cm was used for the irradiations. Dosimeters were placed at four different depths: 2.4, 4.9, 7.4 and 9.9 cm in a 5×5 grid (2 cm between each) covering the central 100 cm^2 of the beam. A total of 100 dosimeters were used at each irradiation. All measured dose values were corrected for the depth dose on the central axis. No correction of the expected dose for off-axis variations was included, due to the small variations ($\pm 1 \%$ ¹⁾. The data was analysed according to the statistical method used in papers III and IV (cf appendix).

¹⁾ Estimated from an exposed film placed at 5 cm depth.

- The estimated coefficient of variation (CV)¹ for the *dose distribution* was 1.4 %. Since all dose values were corrected for the depth variation, the only remaining dose variation is the actual off-axis variation. Thus, the CV value is an estimation of the off-axis variations for all five depths.
- The estimated CV due to the *repeated* treatments was 0.8 %. This value includes contributions from accelerator output differences (e.g. flatness and absorbed dose), set-up inaccuracies, variations in the dosimetry system etc.
- The estimated *residual* CV was 5.8 %. The variations contributing to the total variance that can not be derived from the dose variation or the repetitive treatment are found in the residual variance.
- The *total* CV was 6.1 %.

If the total variance should be used as an estimate of the variance of the *in-phantom* dose distribution instead of the extracted dose distribution variance a considerably higher dose variation should be found. In this case, comparisons with calculations from dose planning systems, where no treatment and dosimetry method related contributions to the variance are present, can not be done on equal terms.

When the dosimeters were placed in the Rando phantom, the influence from the 0.2 cm thick polystyrene slices used for positioning the dosimeters could be neglected according to the results given in figure 8.

The dosimetrical method combined with the statistical analysis for estimation of variance is a tool for identification and control of contributions to the total variance. The measurements in the polystyrene cube and those in paper III and IV all show repetition and residual variances of the same order. It is therefore concluded that the accuracy of the method for determining absorbed doses in an Alderson phantom is of the same order as for the cubic polystyrene phantom.

¹⁾The coefficient of variation is the ratio between one standard deviation and the grand mean value times 100 %.

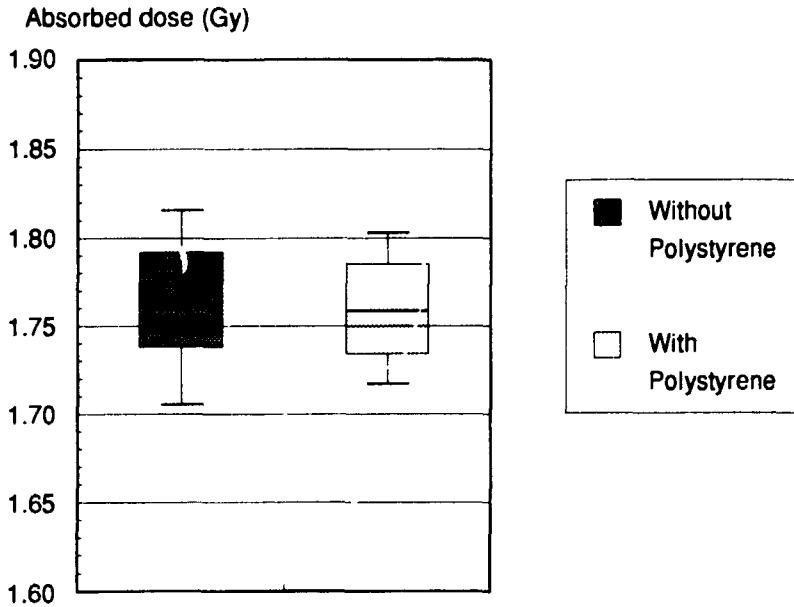


Figure 8: A box plot for the absorbed dose determined by thermoluminescent dosimeters placed inside an anthropomorphic phantom (Alderson Rando Phantom). Six irradiations with two opposed fields (6 MV) were made with and without a 0.2 cm thick polystyrene sheet. The dosimeters were placed in eight holes, diameter 0.5 cm and 0.12 cm deep either in the polystyrene sheet or in the Alderson plastic. The radiation beam axes were parallel to the plane of the dosimeters. The box represents the two central quarters of the distribution of dose values. The thick line in the middle is the median value and the two lines above and under the box represent the 90 and 10 % values of the distribution. The expected mean absorbed dose to the dosimeters was 1.79 Gy. The difference in mean dose between the two groups is less than 0.01 Gy.

APPLICATION OF A DOSE PLAN

A dose plan gives the dose distribution relative to a nominal accelerator output for a reference field. The calibration of accelerators follows one of many protocols (AAPM, CFMRI, DIN, HPA, IAEA, NACP, SEFM) and results in an accelerator output factor, OF_{ACC} expressed as absorbed dose per monitor unit (Gy/MU) for reference dosimetry conditions. However, using other field sizes, wedge filters, shadow blocks etc will change the output. Field factors and correction factors for fluence shaping filters are introduced for this purpose.

The variation in field output factor has until recently mainly been explained as scatter produced in the irradiated phantom (patient). However, a

substantial part is also due to perturbations by photons and electrons scattered from the upper surfaces of the collimators back into the monitor ionization chamber.

Modelling of Energy Fluence from an Accelerator

Generally, the absorbed dose to a point, P in an irradiated object (phantom or patient) relative to the number of monitor units detected by the monitor ionization chamber in the accelerator can be characterized by:

- The absorbed dose at P in the object that the energy fluence Ψ in air at the same point results in. The transport of energy and scatter production in the irradiated object should be handled by the dose calculation process.
- The variation of the energy fluence at P due to perturbations on the detected signal from the monitor chamber, for example, photons back-scattered from the upper side of the collimators and forward scatter from the accelerator head to P . These changes must either be determined experimentally for all collimator settings etc (which is impractical) or be based on modelling as in paper VI.

The model outlined in paper VI for the fluence variations is based on the following assumptions:

- The energy fluence in air at P consist of primary photons, $\Psi_{PRIMARY}$ and photons scattered in the flattening filter and the collimators $\Psi_{SCATTER}$. The energy distributions for $\Psi_{PRIMARY}$ and $\Psi_{SCATTER}$ are assumed to be similar. Only first order processes are considered, Thus, $\Psi_{SCATTER} = \text{constant} \cdot \Psi_{PRIMARY}$
- The signal M from the monitor ionization chamber is a summation of two components — the signal produced by photons, from the target, passing through the chamber, $M_{PRIMARY}$ and the signal produced by photons which are back-scattered in the treatment head and re-enters the chamber.
- The back-scatter originates only from the upper side of the collimator blocks, M_{LOWER} and M_{UPPER} , respectively, and consists of single scattered photons only. The back-scatter from the upper and lower collimator blocks are independent of each other. All other scatter from moving parts (ie which influence M when the collimator setting is changed) is assumed to be included in this term.
- No variable scatter reaches the monitor chamber at maximum field size. Thus, the monitor signal at maximum field size is assumed to be unperturbated.

These assumptions are summarized in the following equation for the relation between the monitor signal and the energy fluence at the reference point P :

$$\frac{M}{\Psi}(l, u) = \frac{M_{PRIMARY} + M_{LCWER} + M_{UPPER}}{\Psi_{PRIMARY} + \Psi_{SCATTER}}$$

where l and u are the settings of the collimator for the lower and upper blocks, respectively. Assuming that no back scatter reaches the monitor at maximum field size, a measurable quantity, the *output perturbation factor*, $m(l, u)$, can be defined as the relative energy fluence per monitor unit normalized to the largest field size:

$$m(l, u) = \frac{\frac{M}{\Psi}(l_{max}, u_{max})}{\frac{M}{\Psi}(l, u)}$$

This expression has been fitted to a small set of measurements of $m(l, u)$ for field sizes with one collimator pair at maximum position while varying the other and repeated with the other pair of blocks at maximum field size. Measurements were made using a thimble ionization chamber covered with 0.3 cm lead to ensure electronic equilibrium and to stop all contaminating electrons from the treatment head etc.

Calculation of Monitor Units

The transfer of the dose plan to the patient can be described as in figure 9. The relative output perturbation factor, $m(l, u)$ is determined together with the model from the geometries (a) and (b) making the fluence variations at P predictable. The absorbed dose per fluence in the patient (d) relative to that for the reference field in the semi-infinite case in (c) is calculated using a dose calculation algorithm, for instance the convolution method in paper II. This ratio is called the *convolution output factor*, OF_{CONV} or generally the dose calculation output factor, OF_{CALC} . The field size, $F(l', u')$ used in the dose calculation is not necessarily the same as that defined by the collimators, $C(l, u)$. For the reference conditions in (c) the accelerator output, OF_{ACC} , is known.

Combining the convolution output factor, $OF_{CONV}(l, u)$ and the output perturbation factor, $m(l, u)$ yields :

$$OF(l, u) = OF_{CONV}(l, u) \cdot m(l, u)$$

The monitor setting, M_{SET} (MU) for a prescribed dose D to the point P can now be calculated:

$$M_{SET} = \frac{D(P)}{OF(l,u) \cdot OF_{ACC}}$$

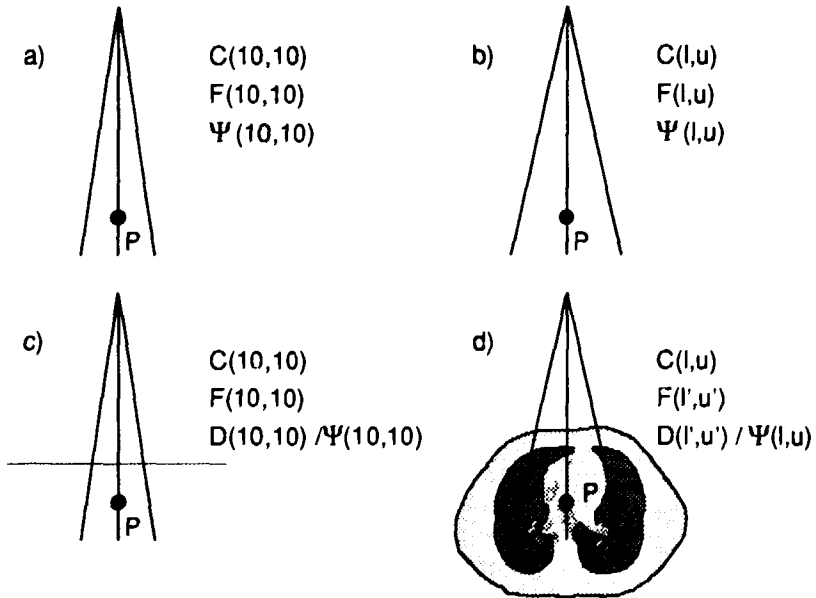


Figure 9: The principles of transferring a dose plan to the treatment situation. a) The energy fluence in air at the reference point (P) per monitor units for a 10 x 10 cm² field. b) Same as a) but for a rectangular field defined by the lower (l) and upper (u) collimator setting. c) The absorbed dose per energy fluence unit for a 10 x 10 cm² field impinging on a semi-infinite water phantom. d) The absorbed dose for a field ($l \times u$) per energy fluence for an irradiated irregular inhomogeneous object. a) and b) are accelerator dependent and c) and d) are dependent on the beam quality and beam shaping and are determined by a dose calculation algorithm.

Output factors were measured in water at 10 cm depth for different positions of the collimator blocks using a thimble ionization chamber. The depth dose measurements in paper V showed for high energy X-rays (18 MV) that a wedge filter acted as an electron filter for those electrons produced in the flattening filter, air column and the collimator. The depth doses decreased in the first centimetres when the wedge filters were in position. Therefore, determinations of output factors as well as wedge attenuation factors were made at a depth larger than the range of the contaminating electrons.

The use of the developed output perturbation factor together with the dose calculation model used in paper VI results in predicted output factors within 1 % of those measured. Commonly, a single combined output factor is used which does *not* separate the variations in the output perturbation and dose calculation factors. Compared with conventional methods using this combined output factor, a significant decrease in the uncertainty of the delivered mean dose to the target volume can be achieved. This is especially pronounced in situations where only quadratic field shapes have been used during the output factor determinations. Furthermore, the use of a convolution output factor will also account for the lack of scatter, for example in situations with tangential beam techniques.

The model requires that the dose calculation algorithm used gives the absorbed dose in the irradiated object relative to the absorbed dose from a reference beam ($10 \times 10 \text{ cm}^2$) impinging on a semi-infinite water phantom. Convolution/superposition models like the method in paper II or the pencil-beam algorithm (Ahnesjö *et al.*, 1990) used in paper VI fulfils this requirement. These methods calculate the absorbed dose relative to the incoming photon fluence (Gy cm^2). The results for clinical situations can therefore be related to the reference geometry.

Results for various accelerators indicate that the output perturbation factor is strongly dependent on the design of the monitor chamber used. Monitor chambers with thin walls are significantly more sensitive to back-scattered radiation than those with thick walls. The energy of the X-ray beam does not seem to influence the magnitude of the back-scatter.

Earlier, accelerators were equipped with thick monitor chambers, but since the specifications for electron beams have changed, thinner monitor chambers have come into use. The effect of using the thinner chambers is clearly seen if the results in paper VI for one of the accelerators is compared with data previously presented by Kubo (1989). Kubo reported a maximum back scatter less than 2 % for both 6 and 18 MV. Our study showed variations in the order of 5-10 %. The inconsistency between the results is directly related to the type of monitor chamber used. The monitor chamber in the accelerator studied by Kubo had an exit window of 0.07 g/cm^2 compared with 0.02 g/cm^2 for the newer type of monitor chamber.

Many accelerators installed today have possibilities to use asymmetrical fields and multileaf collimators. The calculation of monitor units per unit absorbed dose will be more complicated using these devices. The scatter components discussed will be of higher importance in the future, especially when highly asymmetrical collimator settings are used where a much larger

collimator area will be involved. The position of beam shaping devices should be considered during the design of an accelerator in order to keep these perturbations as low as possible.

GENERAL SUMMARY

The use of CT-scanners will improve the accuracy of the given absorbed dose in many ways, but one important contribution is the localization of the target volumes and the surrounding anatomy. The spatial bias of the dose distribution decreases when CT forms the basis for localization and dose planning. However, the results from a CT scan does also include information of the linear attenuation coefficients in the investigated tissues which can be used for dose calculations.

The physical quantity *electron density* is fundamental for both photon and electron dosimetry. In paper I an experimental method for determination of electron densities in materials used as tissues substitutes was reported. These materials were carefully chosen so that their mass attenuation coefficients and their elemental compositions were as close as possible to the tissues. Calibration of CT scanners using these materials has been done, thus enabling the determination of electron density *in vivo*.

The use of accurate mapping of electron density distributions has increased the accuracy for *dose calculation* substantially and has also made it possible to introduce better dose calculation algorithms, for example the method presented in paper II. Such algorithms *require* knowledge of the electron density distribution determined in 3D.

The dose calculation method (paper II) accounts for — in 3D — both the distribution of scattered radiation and the transport of energy by charged particles. The latter will, compared with present methods, increase the accuracy significantly in situations where charged particle disequilibrium exists, for example for narrow beams in low density media. The scatter modelling will also increase the accuracy for treatment techniques where very irregular volumes are included, for example the head and neck region and for tangential treatment of breast cancer.

The effect on the final absorbed dose to the target volume using accurate electron densities combined with an accurate dose calculation method is primarily a decrease in the uncertainty of the mean absorbed dose. However, in situations with large electron density variations, the dose distribution inside as well as outside (organs at risk) of the target volume will be more accurate. Thus, the possibilities to optimize during the dose planning process has been increased which will lead to more advantageous dose distributions.

Objective methods for *verification* of dose distributions is essential. The method outlined in paper III makes it possible to exclude the treatment related variance contributions, making an objective evaluation of dose calculations with experiments feasible.

Careful determination of *output factors* from an accelerator giving input data to an accurate model for prediction of output factors for arbitrary field sizes (paper VI) will considerably decrease the uncertainty when the calculated dose plan is applied clinically. The model for output factors is intimately connected to the convolution dose calculation method (paper II) due to its capability to supply absorbed dose per unit energy fluence. However, it is also possible to apply the method for less sophisticated dose calculations using separate output factors for collimator setting and field size at isocentre.

CONCLUSIONS

The methods discussed and used in this study all contribute to decrease the uncertainty when applying *reference dosimetry* for *treatment execution*. As discussed above, a total uncertainty of 3 to 5 % in the delivered absorbed dose is the goal, but already the uncertainty in the reference dosimetry procedures amounts to 2.5 % (Andreo, 1990). This figure has, however, been obtained combining the uncertainties for several steps in the accelerator calibration chain. For the actual measurement, both Andreo (1990) and Brahme *et al* (1989) proposes uncertainties of 1.0 % for the field instrument reading¹ and 1.5 % for the dose monitor of the accelerator. The latter value is estimated from long time variations of the output from accelerators. However, using modern accelerators with regular quality controls, for example, daily measurement of the output factor, it should be possible to reduce this figure (e.g. to 0.5 %). The figure for the field instrument reading can probably also be decreased using the best available dosimetry equipment. Therefore, a final uncertainty for the reference dosimetry of 2.0 % is assumed.

The total uncertainty in the dose calculations, including all steps discussed in this study, is estimated to between 1 and 4 %. In figure 10, it can be seen that the uncertainty in the dose calculations must be kept low to fulfil the 5 % requirement while still allowing inevitable treatment contributions. The 3 % level can only be reached in situations where the dose calculation and the treatment uncertainties can be kept extremely low. When such high accuracy in the delivered dose is required, the treatment technique used should be chosen with extreme attention shown to the reproducibility of the treatment.

¹Recombination losses, temperature and pressure corrections etc.

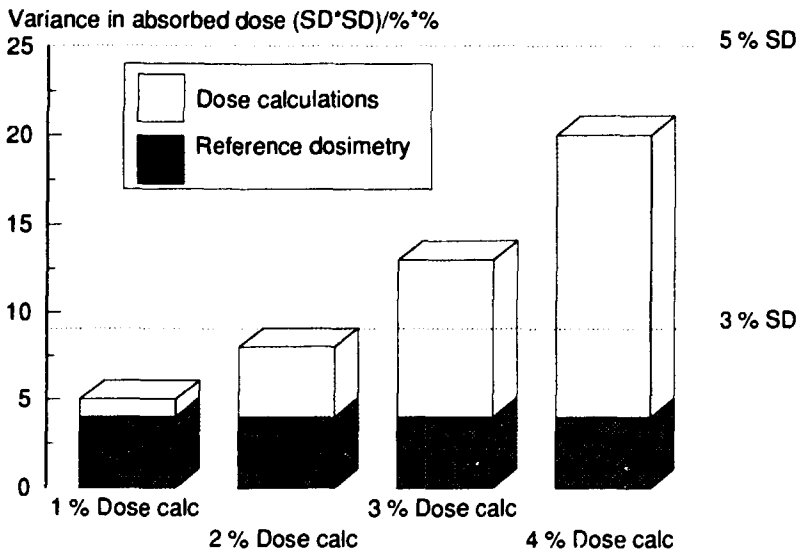


Figure 10: The uncertainties involved in the major steps in the radiation therapy chain before treatment is given. Reference dosimetry (calibration of an accelerator under reference conditions) and dose calculations (dose distributions and absorbed dose per field to be delivered). The height of each bar represents the uncertainty (1 SD, %). The dotted lines shows the 3 and 5 % requirements for the mean absorbed dose to the target volume.

The steps involved in the treatment execution (immobilization, *in vivo* dosimetry, follow-up during treatment etc) must therefore be given the highest priority in the future. Otherwise, what was gained during the reference dosimetry and dose calculation steps may be lost when the treatment is delivered.

FUTURE DEVELOPMENT

The following areas in radiotherapy should, in the author's opinion, in the future be given high priority.

Consistency When Reporting Absorbed Dose

One very important field where efforts are needed is the consistency in dose reporting. If standard nomenclature and principles are used for reporting and describing radiation therapy treatments, tumour/dose response information will be possible to share and compare between treatment centres.

The continuing work to produce *Codes of Practice* and the reference dosimetry data required for determination of absorbed dose, as well as parameters used for description of beam quality, must be fully acknowledged by all those involved in radiotherapy. The uncertainty in the methods for choosing parameters and even in the data used must be reduced.

Dosimetric Methods Used for Verification

Methods for verification of the actual dose distribution inside the patient and in clinically relevant phantoms should be developed and used on a routine basis. The TLD method described in this study is rather cumbersome and faster and more accurate methods should be investigated. One method proposed (Augustsson *et al.* 1984, Jónsdóttir *et al.* 1988) utilizing detectors scanning inside a body shaped phantom filled with water could be used in several clinical situations where the influence from inhomogeneities is negligible. Another promising attempt is to use MRI combined with gelled ferrous-sulphate to measure 3D dose distribution (Olsson *et al.* 1989, Olsson *et al.* 1990). A large step further in verification would be gained if gels of various electron density could be produced. A tool like this would be revolutionary to the quality assurance of dose calculation algorithms and treatment techniques.

Multileaf Collimator

The introduction of multileaf collimators (MLC) will allow conformation of the treated volume to the target volume with limited use of other field shaping devices. The next step is to use the MLC to produce arbitrary dose distributions (Källman *et al.* 1988) determined by inverse treatment planning (Lind and Brahme, 1985). This will probably make it possible to further raise the absorbed dose to the target volume without exceeding the tolerance for surrounding tissues.

On-line Verification

On-line imaging of the volume that is actually treated has recently been shown to be possible (Meertens *et al.* 1985, Lam *et al.* 1986, Leong, 1986, van Herk and Meertens, 1988, Munro *et al.* 1990). The use of these devices for on-line corrections of patient set-up, transmitted dose etc has not yet been clinically evaluated and studies in this field must be initiated in the near future.

The use of on-line verification systems is intimately connected with the MLC for field shaping. It can be foreseen that these devices are going to be connected allowing information from the image system to be fed back on-line to the MLC.

3D-Treatment Planning

A 3D treatment planning system consists of a patient description module, a dose calculation module, and finally a module to view the volumes to be irradiated. The new algorithms can reduce the uncertainties in the dose calculations substantially. Using a system with possibilities to view all target volumes together with the organs at risk, beam limits etc will give the dose planner the potential to create a treatment plan with a high dose to the target volume without reaching the tolerance of the surrounding tissues. Possibilities to use non-coaxial and/or non-coplanar field arrangement will be given.

Treatment Execution

This step in the radiation therapy chain is the one which must be given the highest attention in the future. To start with, the following problems must be dealt with more stringently:

- ☛ Immobilization of the patients in treatment position.
- ☛ Localization of anatomical structures and keeping them as reference points during therapy, including CT-scanning, dose planning and treatment execution.
- ☛ Set-up and verification of the beam orientation at the simulator for non-coplanar and non-axial techniques.

ACKNOWLEDGEMENTS

A lot of other people have been involved, it is shaky to put down their names, because somebody will probably be forgotten, but here they are:

Mats Nilsson, my main scientific supervisor to whom I express my sincere gratitude for his support and encouragement.

Lars Ahlgren, scientific supervisor

Sören Mattsson, who gave me the possibilities to write this thesis.

The following senior physicists and physicians who taught me the basics of radiotherapy:

Nils-Erik Augustsson, Torsten Landberg, Ulla-Brita Nordberg, Gudrun Svahn-Tapper

The group at the Department of Radiation Physics at Lund University who fooled me into this thing called science a long time ago.

And all these people who have struggled with the TLD's.

Karin Martling, Kristina Berndtson, Kai Nilsson, Christel Andersson

A special THANK YOU to Lena Wittgren who have helped me with the measurements for some of the papers, valuable discussions and doing the hospital duties during my absence for the completion of this thesis.

Anders Ahnesjö for fruitful and stimulating discussion and collaboration.

Last but not least, the people who actually perform all these treatments. If it was not for them, all discussions regarding accuracy is inappropriate. It is their skill and care at the accomplishment of the treatments that gives the final result.

I will also express my gratitude to all other at the Departments of Radiation Physics and Oncology at Malmö Allmänna Sjukhus.

Financial support for parts of the studies included in this thesis have been received from:

Medicinska Forskningsrådet

Allmänna sjukhusets i Malmö stiftelse för bekämpande av cancer

John och Augusta Persson stiftelse för vetenskaplig medicinsk forskning

APPENDIX

Equations used for the estimation of variances contributions:

The measured value, x_{ij} , is the measured absorbed dose at position i (1.. k positions) in the phantom at the j -th measurement (1.. n measurements). Each x is assumed to be an estimate of the following variable:

$$x_{ij} = \bar{m} + \varepsilon_i + \zeta_j + \delta_{ij}$$

where \bar{m} is the mean value, ε is the contribution due to repetitive treatments, ζ is the contribution from the actual dose distribution and δ is the residual contribution. Both the ε , ζ and the δ contributions have expectation values equal to zero.

The estimated variances, s_i are calculated using the following sum of squares:

$$S_T = \sum_{i=1}^k \sum_{j=1}^n x_{ij}^2 - \bar{x}^2$$

$$S_L = \sum_{i=1}^k \frac{\left(\sum_{j=1}^n x_{ij} \right)^2}{n} - \bar{x}^2$$

$$S_C = \sum_{j=1}^n \frac{\left(\sum_{i=1}^k x_{ij} \right)^2}{k} - \bar{x}^2$$

The total, the repetition, the distribution and the residual (0) variances are then estimated by:

$$s_{total}^2 = \frac{S_T}{kn - 1}$$

$$s_{repetition}^2 = \frac{1}{n} \cdot \left[\frac{S_L}{k - 1} - s_0^2 \right]$$

$$s_{distribution}^2 = \frac{1}{k} \cdot \left[\frac{S_C}{n - 1} - s_0^2 \right]$$

$$s_0^2 = \frac{1}{(k - 1)(n - 1)} \cdot [S_T - S_L - S_C]$$

REFERENCES

- AAPM, American Association of Physicists in Medicine, A protocol for the determination of absorbed dose from high-energy photon and electron beams, *Med Phys*, 10, 741-771, 1983.
- Ahnesjö A, Collapsed cone convolution of radiant energy for photon dose calculation in heterogeneous media, *Med Phys*, 16, 577-592, 1989.
- Ahnesjö A, Saxner M, Trepp A, A pencil beam model for photon dose calculations, Submitted to *Medical Physics*, 1990.
- Ahnesjö A, Andreo P, Brahme A, Calculation and application of point spread functions for treatment planning with high energy photon beams, *Acta Oncol*, 26, 49-56, 1987.
- Andreo P, Uncertainties in dosimetric data and beam calibration, *Int J Radiation Oncology Biol Phys*, 19, 1233-1247, 1990.
- Augustsson N-E, Nilsson M, Westerlund K, A new instrument for measurement of absorbed dose inside an irregular volume, In: Abstract from the 42:nd Nordic Radiology Congress, Malmö (In Swedish), 1984.
- Batho H F, Lung corrections in cobalt 60 beam therapy, *J Canadian Ass Radiologists*, 15, 79-83, 1964.
- Beaudoin L, Analytical approach to the solution of dosimetry in heterogeneous media, M Sc Thesis, University of Toronto, Canada, 1968.
- Berger M J, Hubbell J H, XCOM: Photon cross sections on a personal computer, Report No. NBSIR 87-3597, US Government Printing Office, Washington, D C., 1987.
- Björngård B E, Kase K R, Rudén B-I, Biggs P J, Boyer A L, Johansson K A, Postal intercomparison of absorbed dose for high energy X-rays with thermoluminescence dosimeters, *Med Phys*, 7, 560-565, 1980.
- Boyer A, Shortening the calculation time of photon dose distributions in an inhomogeneous medium, *Med Physics*, 11, 552-554, 1984.
- Boyer A L, Zhu Y, Wang L, Francis P, Fast Fourier transform convolution calculations of X-ray isodose distributions in homogeneous media, *Med Phys*, 16, 248-253, 1989.
- Boyer A, Mok E, A photon dose distribution model employing convolution calculations, *Med Phys*, 12, 169-177, 1985.
- Brahme A, Chavaudra J, Landberg T, McCullough E C, Nüsslin F, Rawlinson A, Svensson G, Svensson H, Accuracy requirements and quality assurance of external beam therapy with photons and electrons, *Acta Oncol Suppl* 1, 1988.
- Brahme A, Dosimetric precision requirements in radiation therapy, *Acta Radiol Oncol*, 23, 379-391, 1984.
- CFMRI, Comité Français Mesure des Rayonnements Ionisants, Recommendations pour la détermination de la dose absorbée en radiothérapie dans les faisceaux de photons et d'électrons d'énergie comprise entre 1 MeV et 50 MeV, Rapport CFMRI No 2, 1984.
- Cunningham J R, Scatter-Air ratios, *Phys Med Biol*, 17, 42-51, 1972.
- Cunningham J R, Tissue inhomogeneity corrections in photon-beam treatment planning, In: *Progress in medical radiation physics vol 1*, Ed. Orton C G, Plenum, New York, 103-131, 1982.
- DeVita V, Progress in cancer management: Keynote address, *Cancer*, 51, 2401-2409, 1983.
- DIN, Deutsches Institut für Normung, Dosimessverfahren in der radiologischen technik-Ionisations dosimetrie, Manuskript DIN 6800 Teil 2, 1980.
- Dobbs H J, Parker R P, Hodson N J, Hobday P, Husband J E, The use of CT in radiotherapy treatment planning, *Radioth Oncol*, 1, 133-142, 1983.

- Dutreix A, When and how can we improve precision in radiotherapy?, *Radioth Oncol*, 2, 275-292, 1984.
- Evans R D, *The Atomic Nucleus*, McGraw-Hill, 1955.
- Fano U, 1954, Note on the Bragg-Gray cavity principle for measuring energy dissipation. *Radiation Res.* 1, 237.
- Goitein M, Applications of CT in radiotherapy treatment planning, In: *Progress in medical radiation physics vol 1*, Ed. Orton C G, Plenum, New York, 195-293, 1982.
- HPA, Hospital Physicists Association, Revised code of practice for the dosimetry of 2 to 25 MV X-ray and of caesium-137 and cobalt-60 gamma-ray beams, *Phys Med Biol*, 28, 1097-1104, 1983.
- Hubbell J H, Veigele W M J, Briggs E A, Brown R T, Cromer D T, Howerton R J, Atomic form factors, incoherent scattering functions and photon scattering cross sections, *J Phys Chem Ref Data*, 4, 471-538, 1975.
- IAEA, International Atomic Energy Agency, Absorbed dose determination in photon and electron beams. An international code of practice, Technical reports series no 277, Vienna, 1987.
- ICRU, International commission on radiation units and measurements, No 24: Determination of absorbed dose in a patient irradiated by beams of X or gamma rays in radiotherapy procedures, Bethesda, Maryland, USA, 1976.
- ICRU, International commission on radiation units and measurements, No 29: Dose specifications for reporting external beam therapy with photons and electrons, Bethesda, Maryland, USA, 1978.
- ICRU, International commission on radiation units and measurements, No 33: Radiation quantities and units, Bethesda, Maryland, USA, 1980.
- ICRU, International commission on radiation units and measurements, No 44: Tissue substitute in radiation dosimetry and measurement, Bethesda, Maryland, USA, 1989.
- Johansson K-A, Mattsson L O, Svensson H, Dosimetric intercomparison at the Scandinavian radiation therapy centres. 1. Absorbed dose intercomparison, *Acta Radiol Oncol*, 21, 1-10, 1982.
- Johansson K-A, Horiot J C, Van Dam J, Lepinoy D, Sentenec I, Sernbo G, Quality assurance control in the EORTC cooperative group of radiotherapy. 2. Dosimetric intercomparison, *Radioth Oncology*, 7, 269-279, 1986.
- Jónsdóttir T, Augustsson N-E, Nilsson M, Dose measurements in an irregular breast phantom, M Sc Thesis, RADFYS 88:4, Lund University, Dept radiation physics, Malmö Allmänna Sjukhus, S-214 01 Malmö, SWEDEN (In Swedish), 1988.
- Knöös T, Nilsson M, Calculation of 3D dose distributions for photons in inhomogeneous media, In 'The use of computers in radiation therapy', Proc Ninth International Conference on the Use of Computers in Radiation Therapy, Ed Bruinvis IAD, North-Holland, 1987.
- Knöös T, Weekly output measurements for accelerators: Results for 1987, RADFYS 88:1, Lund University, Dept radiation physics, Malmö Allmänna Sjukhus, S-214 01 Malmö, SWEDEN (In Swedish), 1988.
- Kubo H, Telescopic measurements of back-scattered radiation from secondary collimator jaws to a beam monitor chamber using a pair of slits, *Med Phys*, 16, 295-298, 1989.
- Källman P, Lind B, Eklöf A, Brahme A, Shaping of arbitrary dose distributions by dynamic multileaf collimation, *Phys Med Biol*, 33, 1291-1300, 1988.
- Lam K-S, Partowmah M, Lam W-C, An on-line electronic portal imaging system for external beam radiotherapy, *Brit J Radiology*, 59, 1007-1013, 1986.
- Landberg T, Personal communication, 1991.

- Leong J, Use of digital fluoroscopy as on-line verification device in radiation therapy, *Phys Med Biol*, 31, 985-992, 1986.
- Lind B, Brahme A, Generation of desired dose distributions with scanned elementary beams by deconvolution methods, In *Proceedings from: XIV ICMBE and VII ICMP - Espoo - Finland*, #, #, 1985.
- Lulu B A, Bjärngard B E, Batho's correction factor combined with scatter summation, *Med Phys*, 9, 372-377, 1982.
- Mackie T R, El-Khatib E, Battista J, Scrimger J, Van Dyk J, Cunningham J R, Lung dose corrections for 6 and 15 MV X-rays, *Med Phys*, 12, 327-332, 1985a.
- Mackie T R, Scrimger J W, Battista J J, A convolution method of calculating dose for 15 MV X-rays, *Med Phys*, 12, 188-196, 1985b.
- Meertens H, van Herk M, Weeds J, A digital image detector for treatment field verification of high energy photon beams, In *Proceedings from: XIV ICMBE and VII ICMP - Espoo - Finland*, #, #, 1985.
- Metcalfe P E, Hoban P W, Murray D C, Round W H, Beam hardening of 10 MV radiotherapy x-rays: analysis using a convolution/superposition method, *Phys Med Biol*, 35, 1533-1549, 1990.
- Metcalfe P E, Hoban P W, Murray D C, Round W H, Modelling polychromatic high energy photon beams by superposition, *Austral Phys Eng Sci Med*, 12, 138-148, 1989.
- Mijnheer B J, Batterman J J, Wambersie A, What degree of accuracy is required and can be achieved in photon and neutron therapy?, *Radioth Oncol*, 8, 237-252, 1987.
- Mohan R, Chui C, Lidofsky L, Differential pencil beam dose computation model for photons, *Med Phys*, 13, 64-73, 1986.
- Munro P, Rawlinson J A, Fenster A, A digital fluoroscopic imaging device for radiotherapy localization, *Int J Radiation Oncol Biol Phys*, 18, 641-649, 1990.
- NACP, Nordic Association of Clinical Physics, Procedures in external radiation therapy between 1 and 50 MeV, *Acta Radiol Oncol*, 19, 55-79, 1980.
- Nelson W R, Hirayama H, Rogers D W O, The EGS4 code system, Stanford linear accelerator report SLAC-265, 1985.
- O'Connor J E, The variation of scattered X-rays with density in an irradiated body, *Phys Med Biol*, 1, 352-369, 1957.
- O'Connor J E, The density scaling theorem applied to lateral electronic equilibrium, *Med Phys*, 11, 678-680, 1984.
- Olsson L E, Fransson A, Ericsson A, Mattsson S, MR imaging of absorbed dose distributions for radiotherapy using ferrous sulphate gels, *Phys Med Biol*, 35, 1623-1631, 1990.
- Olsson L E, Peterson S, Ahlgren L, Mattsson S, Ferrous sulphate gels for determination of absorbed dose distributions using MRI technique: basic studies, *Phys Med Biol*, 34, 43-52, 1989.
- Purdy J A, Harms W B, Gerber R L, Report on a long-term quality assurance program, In: *Radiation oncology physics, 1986 Summer school, American Association of Physicists in Medicine*, Ed: Kereiakes J G, Elson H R, Born C G, AAPM Medical physics monograph no 15, 91-109, 1987.
- Raeside D E, Monte Carlo principles and applications, *Phys Med Biol*, 21, 181-197, 1976.
- SEFM, Sociedad Espanola de Fisica Medica, Procedimientos recomendados para la dosimetria de fotones y electrones de energias comprendidas entre 1 MeV y 50 MeV en radioterapia de haces externos, SEFM no 1, 1984.
- Sontag M R, Cunningham J R, The equivalent tissue-air ratio method for making absorbed dose calculations in a heterogeneous medium, *Radiology*, 129, 787-794, 1978.
- Suit H D, Phil D, Becht J, Leong J, Stracher M, Wood W C, Verhey L, Goitein M, Potential for improvements in radiation therapy, *Int J Radiation Oncol Biol Phys*, 14, 777-786, 1988.

- Suit H D, Phil D, Miralbell R, Potential impact of improvements in radiation therapy on the quality of life and survival, *Int J Radiation Oncol Biol Phys*, 16, 891-895, 1989.
- Svensson H, Dosimetric measurements at the Nordic medical accelerators II. Absorbed dose measurements, *Acta Radiol Ther Phys Biol*, 10, 631-654, 1971.
- Svensson H, Hanson G P, Zsdánszky K, The IAEA/WHO TL dosimetry service for radiotherapy centres 1967-1987, *Acta Oncologica*, 29, 461-467, 1990.
- van Herk M, Meertens H, A matrix ionisation chamber imaging device for on-line patient set-up verification during radiotherapy, *Radioth Oncol*, 11, 369-378, 1988.
- Wambersie A, Landberg T, Johansson K A, Dobbs J, Gérard J P, Sentenac I, Dose prescription and specification in external radiotherapy: Evaluation of ICRU report 29 and new trends, In: *ICRU NEWS*, Bethesda, Maryland, USA, 2, 25-27, 1989.
- White D R, An analysis of the Z dependence of photon and electron interactions, *Phys Med Biol*, 22, 219-228, 1977.
- White D R, Constantinou C, Anthropomorphic phantom materials, In: *Progress in medical radiation physics vol 1*, Ed. Orton C G, Plenum, New York, 133-193, 1982.
- White D R, Martin R J, Darlinson R, Epoxy resin based tissue substitutes, *Br J Radiol*, 50, 814-821, 1977.
- Wong J W, Henkelman R M, A new approach to CT pixel-based photon dose calculations in heterogeneous media, *Med Phys*, 10, 199-208, 1983.